14 Dec 2011

Effect of Thin Film Confined between Two Dissimilar Solids on Interfacial Thermal Resistance

Zhi Liang
Missouri University of Science and Technology, zlch5@mst.edu

Hai-Lung Tsai
Missouri University of Science and Technology, tsai@mst.edu

Recommended Citation

Z. Liang and H. Tsai, "Effect of Thin Film Confined between Two Dissimilar Solids on Interfacial Thermal Resistance," *Journal of Physics Condensed Matter*, vol. 23, no. 49, article no. 495303, IOP Publishing, Dec 2011.
The definitive version is available at https://doi.org/10.1088/0953-8984/23/49/495303

Effect of thin film confined between two dissimilar solids on interfacial thermal resistance

J. Phys.: Condens. Matter **23** (2011) 495303 (9pp) doi:10.1088/0953-8984/23/49/495303

Effect of thin film confined between two dissimilar solids on interfacial thermal resistance

Zhi Liang and Hai-Lung Tsai

Department of Mechanical and Aerospace Engineering, Missouri University of Science and Technology, 400 West 13th Street, Rolla, MO 65409, USA

E-mail: tsai@mst.edu

Received 5 September 2011, in final form 18 October 2011
Published 22 November 2011
Online at stacks.iop.org/JPhysCM/23/495303

Abstract

A non-equilibrium molecular dynamics model is developed to investigate how a thin film confined between two dissimilar solids affects the thermal transport across the material interface. For two highly dissimilar (phonon frequency mismatched) solids, it is found that the insertion of a thin film between them can greatly enhance thermal transport across the material interface by a factor of 2.3 if the thin film has one of the following characteristics: (1) a multi-atom-thick thin film of which the phonon density of states (DOS) bridges the two different phonon DOSs for the solid on each side of the thin film; (2) a single-atom-thick film which is weakly bonded to the solid on both sides of the thin film. The enhanced thermal transport in the single-atom-thick film case is found mainly due to the increased inelastic scattering of phonons by the atoms in the film. However, for solid–solid interfaces with a relatively small difference in the phonon DOS, it is found that the insertion of a thin film may decrease the thermal transport.

(Some figures may appear in colour only in the online journal)

1. Introduction

With the rapid progress in fabrication technology, many nanoscale structures such as semiconductor superlattices, multi-layer coatings and polymer nanocomposites have been widely used in advanced devices. Thermal management is a serious issue in the application of nanostructures [1]. Due to the high surface-to-volume ratio in nanostructured components and devices, the thermal transport at material interfaces often dominates the overall thermal behavior. In general, thermal resistance across a solid(A)/solid(B) interface is strongly affected by the difference in phonon density of states (DOS) between the solids, and the difference is qualitatively determined by the ratio of the Debye temperatures of the two solids [2]. When the Debye temperature for solid A differs greatly from that for solid B, which will be referred to as dissimilar or phonon frequency mismatched solids in this paper, there will be a large difference in phonon DOS. The large difference in phonon DOS normally results in poor thermal transport across the interface. As an example, it was measured from experiments [3] that at room temperature the thermal resistance at the Au/sapphire interface is about 2×10^{-8} m^2 K W^{-1}, while the Debye temperature differs between Au and sapphire by a factor of 6. In this case, the interfacial thermal resistance is equivalent to the thermal resistance of a 6 μm-thick Au film. An interface with such a high thermal resistance plays a critical role in nanoscale thermal transport. In addition to the difference in phonon DOS, the interfacial thermal resistance is also affected by many other factors such as temperatures and interfacial conditions. To explain the thermal transport phenomena at different kinds of solid–solid interfaces, a variety of theoretical and numerical models have been proposed in the past decade [2, 4–9].

As compared to the acoustic mismatch model (AMM), the diffuse mismatch model (DMM) and the lattice dynamics (LD) model, the molecular dynamics (MD) simulation method is a more realistic model in investigating the thermal transport mechanism since the MD simulation method

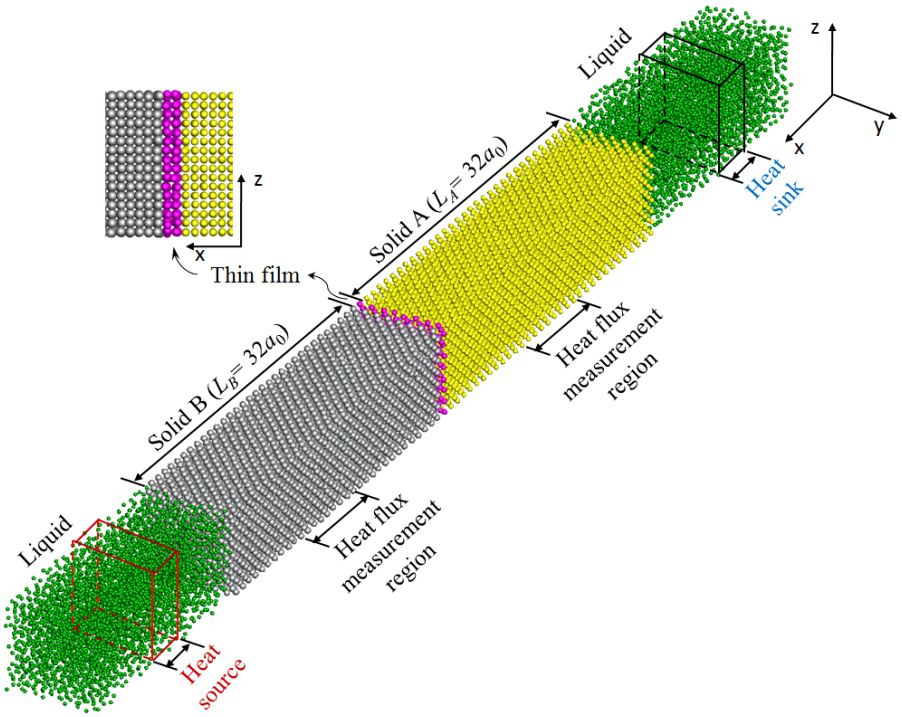

Figure 1. (a) Schematic diagram of a typical simulation system which contains a solid(A)/film/solid(B) structure confined by a liquid bath at a temperature of 1.25 and density of 0.84. The size of each solid slab is $32a_0 \times 8a_0 \times 8a_0$. The length of each liquid slab is about 34. PBCs are applied in three directions. The inset shows a snapshot of a thin film which contains two atomic layers.

accounts for both the elastic and inelastic scattering of phonons at the solid–solid interface and is able to build well-controlled interfaces at the atomic level [1, 2, 5, 7–9]. For instance, a temperature dependent thermal resistance at the solid–solid interface was observed in MD simulations [2, 7]. The decrease in interfacial thermal resistance with increasing temperature agrees with experimental results [10] and is attributed to the increase of inelastic phonon scattering at the interface. For highly mismatched interfaces, it was found from MD simulations [2, 5] that mixing of the two solid materials at the interface can significantly reduce the interfacial thermal resistance. The reduction is also attributed to the increased inelastic phonon scattering which is not accounted for by AMM, DMM or LD models [2]. Most MD simulations of the thermal transport across solid(A)/solid(B) interfaces were carried out in a system where the two solids are in direct contact with each other. In this work, a non-equilibrium MD model is developed to investigate how a thin film confined between two dissimilar solids affects the thermal transport across the material interface.

Thin films with thickness as small as 1 nm exist in many advanced technological devices such as quantum cascade lasers and field effect transistors [11–13]. The technology of soldering submicron-sized electrical contacts to a single atomic layer has also been developed [14]. The thermal transport properties of thin films are being studied since they have the potential to increase the efficiency of many energy conversion devices [9]. Recently, the thermal transport across interfaces in a solid/film/solid structure has been studied by MD simulations [9, 15]. In the simulation, a thin film with the thickness of a few atomic layers is confined between two solid slabs. The two solid slabs are made of the same material which is different from the thin film material. It was found that the interfacial thermal resistance decreases rapidly with decreasing film thickness. Inspired by this result, we consider if it is possible to significantly reduce the thermal resistance at the interface of two dissimilar materials by inserting a thin film between them. In this work, therefore, we study the thermal transport across a solid(A)/film/solid(B) structure by MD simulations and compare R_F, the thin film thermal resistance, to R_S, the thermal resistance at the solid(A)/solid(B) interface. The objective of this study is to find appropriate film properties to improve thermal transport across a phonon frequency mismatched interface. The R_F dependence on film thickness and the film–solid binding strength are investigated. Only thermal transport by phonons is considered in this work. Since phonons are the primary thermal energy carriers in most semiconductors, the simulation results are more applicable to the thermal transport in semiconductor nanostructures.

2. MD model

The schematic diagram of a system which simulates the thermal transport across a solid(A)/film/solid(B) structure is depicted in figure 1. The system consists of two solid slabs which sandwich a thin film. The whole solid(A)/film/solid(B) structure is confined by a liquid bath. The liquid bath is included in the system only for numerical reasons which will be explained later in this section. The atoms in each solid slab are arranged into a [1 0 0]-oriented perfect fcc

crystal with 32 unit cells in the x-direction and 8 unit cells in each of the y- and z-directions. Simulations were also performed on larger structures, but no noticeable difference in simulation results was observed. The initial atomic structure in the thin film is the same as that in the solid slab except that the thin film contains only a few atomic layers in the x-direction. Periodic boundary conditions (PBCs) are applied in all three directions. All inter-atomic interactions are modeled by the Lennard-Jones (LJ) 12-6 potential $E_p(r) = 4\varepsilon[(\sigma/r)^{12} - (\sigma/r)^6]$. In this work, the general effects of thin film on interfacial thermal transport are of interest. The LJ potential is used to account for the general aharmonic nature of real materials [2, 6, 7]. More realistic potentials are planned to be used in the future for specific materials.

The liquid–liquid and solid–liquid interactions are modeled by the LJ potential with parameters (ε, σ) and (ε_{SL}, σ), respectively. Note the magnitude of the potential well depth, ε, represents the binding strength. Since in this simulation the solid(A)/solid(B) interface is far away from the solid/liquid interface, the solid–liquid interaction will not affect the thermal resistance at the solid(A)/solid(B) interface. Hence, we simply set the solid–liquid binding strength $\varepsilon_{SL} = \varepsilon$. The liquid mass is equal to m and the reduced units based on m, ε and σ of liquid are used throughout in this study. The LJ potential for the solid(A)–solid(A) interaction and solid(B)–solid(B) interaction is given by (ε_A, σ) and (ε_B, σ). The Lorentz–Berthelot mixing rule is employed to calculate the LJ parameters for solid(A)–solid(B) interactions.

To study the effect of thin film on the thermal transport, we need to assign potential parameters for solid(A)–film, solid(B)–film and film–film interactions and also assign the film thickness. The thin film thermal resistance, R_F, actually depends on all these parameters. In this work, however, we are interested in investigating the influence of the film thickness and the film–solid binding strength on the R_F. To save the total computational cost, therefore, we assume the film–solid binding strengths are the same as the film–film binding strength in the simulation. And the film–film binding strength is always set smaller than the solid–solid binding strengths ε_A and ε_B. Accordingly, the film–solid and film–film interactions are modeled by the LJ potential with the same parameters (ε_F, σ), where ε_F is less than the ε_A and ε_B. The masses of the atoms in solid(A), solid(B), and thin film are m_A, m_B, and m_F, respectively. The lattice constants of solid(A), solid(B) and thin film are all set to the same value $a_0 = 1.56\sigma$ which is approximately the lattice constant of a fcc lattice at equilibrium. Therefore, there is no lattice mismatch in the simulation system and the effects of interface strain or distortion on thermal transport are not taken into account in this model. To create the phonon frequency mismatch between different materials, we vary the potential well depths ε_A, ε_B, and ε_F or the atomic masses m_A and m_B in the simulation.

Before a heat source and a heat sink are applied to produce temperature gradients in the system, the whole simulation system is equilibrated for a reduced time period of 200 to ensure the desired temperature is reached. We integrate the equations of motion using a velocity Verlet scheme with a reduced time step size of 0.003. The Berendsen *et al*'s algorithm [16] with a reduced time constant of 0.3 is used in the equilibrium MD simulation. The length of the liquid bath is adjusted to let the density of liquid reach the desired value. Using the liquid bath, the simulation can always be performed at the same temperature and pressure. The cut-off radius for all interactions is 2.5 σ. The lattice constants of solids and thin film are fixed at a_0 in the direction parallel to the interface during the equilibration. The temperature and density of liquid are equilibrated to the reduced values of 1.25 and 0.84, respectively. Therefore, the lattice constants of solids and thin film in the direction perpendicular to the interface are relaxed to appropriate values so that the stress in the heat flux direction can always reach the same value no matter what potential parameters or masses are assigned to the solids or the thin film.

Following equilibration, the thermostat is removed and a heat source and a heat sink are applied in the liquid region as depicted in figure 1. The total number of liquid atoms included in the system is 8704. The length of liquid slab on each side of the solid(A)/film/solid(B) structure is about 34 in reduced unit. Each liquid slab is divided evenly into 13 slices in the x-direction. The middle three slices in each of the two liquid slabs are set as the heat source or heat sink. In the non-equilibrium MD simulation, a constant energy ΔE is added to the energy of the atoms in the heat source and is subtracted from the energy of the atoms in the heat sink at each time step by using the Jund and Jullien's method [17]. Since the simulation system is not symmetric with respect to the heat source or heat sink, the heat fluxes flowing out from the heat source in the positive and in the negative x-directions are not equal. Hence, the heat flux q_S across the solid(A)/film/solid(B) structure needs to be obtained from the simulation. In the simulation, each of the two solid slabs is divided evenly into 16 slices in the x-direction with each slice containing four atomic layers. As shown in figure 1, the middle four slices in each of the two solid slabs are set as the heat flux measurement (HFM) region. To evaluate the average phonon heat flux q_S, the following equation is used for the calculation [18].

$$q_S = \frac{1}{V}\left[\sum_i E_i v_{x,i} + \frac{1}{2}\sum_i \sum_j x_{ij}^* (\vec{v}_i \cdot \vec{F}_{ij})\right] \qquad (1)$$

In equation (1), V is the volume of an HFM region, E_i is the sum of the kinetic energy and potential energy of atom i, $v_{x,i}$ is the velocity of atom i in the x-direction, and $\vec{F}_{ij}$ denotes the inter-atomic force. The first term on the right-hand side of equation (1) is a summation over all atoms in the HFM region. The double summation in the second term is over all pairs of atoms with the condition that the line connecting the two atoms is contained or partially contained in the HFM region. Accordingly, x_{ij}^* in equation (1) is the x-component of the whole connecting vector or the portion of the connecting vector contained in the HFM region.

In the non-equilibrium MD simulation, a total heat flux of 0.16 in reduced units is applied to the simulation system for a reduced time period of 1200 to allow the system to reach a steady state. Subsequently, the non-equilibrium MD

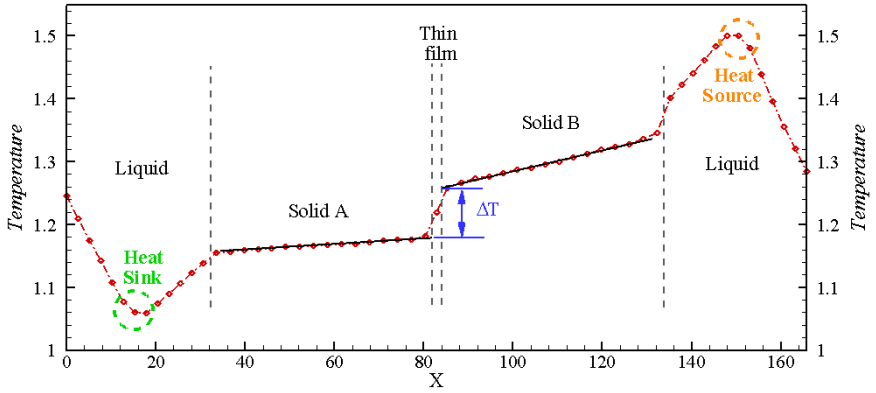

Figure 2. Temperature profile in the x-direction of the simulated system in which the thin film contains two atomic layers and $\varepsilon_F = 1$. All quantities are in reduced units. The uncertainty of temperature is less than the size of the symbols.

simulation is carried out for another reduced time period of 4000 for data collection and averaging. At each time step, the temperature of each solid or liquid slice is calculated. The temperature of the thin film and the heat flux in solid HFM regions are also calculated. At the steady state, the average heat flux in each of the two solid HFM regions becomes almost identical, and their average value is used to evaluate the heat flux across the material interface. Using the block average method [19], the statistical uncertainties of the calculated temperature and heat flux are estimated to be $\pm 0.2\%$ and $\pm 2.5\%$, respectively. In section 3, all physical quantities are given in reduced units. All MD simulations in this work are performed at the reduced temperature of 1.25.

3. Simulation results

3.1. Thermal resistance at the highly mismatched interface

We firstly consider a system containing two solid materials with highly mismatched phonon frequencies. We set $\varepsilon_A = \varepsilon_B = 5$, $m_A = 1$ and $m_B = 9$ such that the simulation temperature ($T = 1.25$) is about one-half of the melting temperature of the two solid materials [2]. As the frequency of the atomic vibration is proportional to the square root of potential well depth over atomic mass, the high phonon frequency mismatch is achieved by setting a high mass ratio ($m_B/m_A = 9$) in this simulation. Thus, $\sqrt{(\varepsilon_B/m_B)/(\varepsilon_A/m_A)} = 0.33$. For the thin film material, we fix $m_F = 2$ and vary the film–film and film–solid binding strengths by setting $\varepsilon_F = 0.25$, 0.5, 1, 2 or 4 such that $\sqrt{(\varepsilon_F/m_F)/(\varepsilon_A/m_A)} = 0.16$, 0.22, 0.32, 0.45 or 0.63. Therefore, the variation of phonon frequency mismatch between thin film and solid A is achieved by changing ε_F in the simulation. Additionally, we vary the thickness of the thin film from one-atom-thick to four-atoms-thick to investigate the influence of film thickness on thermal transport across the interface.

A typical temperature profile in the x-direction of the simulated system is shown in figure 2. The results shown in figure 2 are obtained when the thin film contains two atomic layers with $\varepsilon_F = 1$. It can be seen that the temperature profiles in the two solids are almost linear. The temperature gradient in solid B is larger than that in solid A, which indicates solid A has a higher thermal conductivity. In the simulation, we apply the method of linear least squares to the temperature profile in each solid slab and evaluate the linear fits at the two solid/film interfaces to determine the temperature difference ΔT as depicted in figure 2. Note the temperature points most adjacent to the interfaces are ignored in the linear fit process since the temperature distribution near the interfaces is generally nonlinear. The thin film thermal resistance R_F is determined by equation (2).

$$R_F = \Delta T/q_S \tag{2}$$

where q_S is the heat flux across the thin film which is determined by equation (1). In this set of simulations, the measured q_Ss for different thin film parameters are mostly around 0.052. The same method is applied to calculate R_S, the thermal resistance at the solid(A)/solid(B) interface. In the calculation of R_S, ΔT is determined from the difference of the linear fits of temperature profiles in solid A and solid B at the solid(A)/solid(B) interface. By repeating the simulation with four independent random seed values and performing error propagation analyses [2], we find the uncertainty of ΔT in most simulation runs is less than 3%, and the uncertainty of thermal resistance is typically less than 4%. When solid A is in direct contact with solid B, it is found that $R_S = 2.03$ for an atomically perfect interface. When a thin film is inserted between solid A and solid B, R_F as a function of ε_F and film thickness is shown and compared to R_S in figure 3.

The ratios of R_F to R_S as a function of film thickness for fixed ε_Fs are shown in figures 3(a) and (b). For all fixed ε_Fs, it is found that R_F always decreases to a value considerably lower than R_S and then increases as the number of atomic layers in the thin film increases (for $\varepsilon_F = 4$, the R_F and R_S ratio starts to increase after the fourth layer, not shown in the figure). If ε_F is equal to 1 or lower (relatively low ε_Fs as compared to the simulation temperature which is 1.25), R_Fs reaches the minimum when there is only one atomic layer in the thin film. For $\varepsilon_F = 2$ and 4, R_Fs reaches the minimum when there are, respectively, two and four atomic layers in the thin film. Figure 3(c) shows R_F as a function of ε_F for thin films with a fixed number of atomic layers. It is

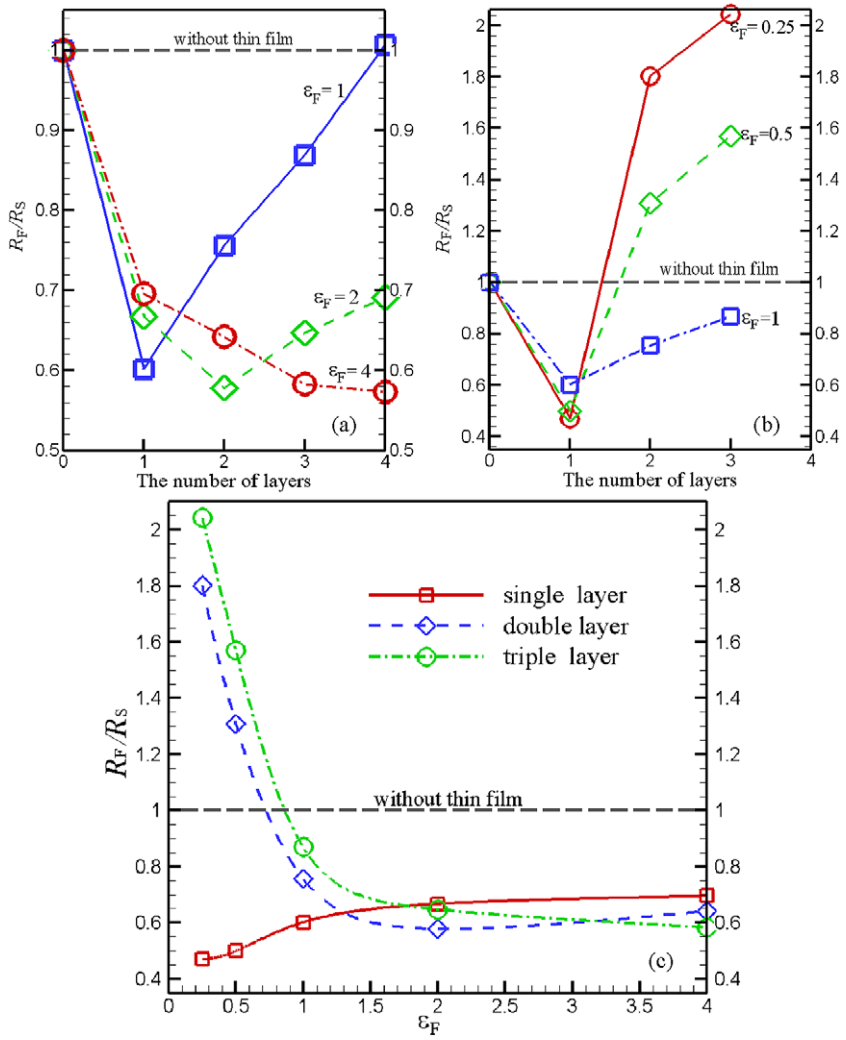

Figure 3. Thin film thermal resistance as a function of film thickness for (a) $\varepsilon_F = 1$, 2 or 4; (b) $\varepsilon_F = 0.25$, 0.5 or 1; and (c) thin film thermal resistance as a function of ε_F for a highly mismatched interface whose $R_S = 2.03$. The uncertainty of R_F is less than the size of the symbols.

seen that R_F versus ε_F curves show totally different behaviors for single-layer film and multi-layer films. If the thin film contains only one atomic layer, it is found in figure 3(c) that R_F increases with ε_F, which indicates that the lower film–solid binding energies will result in a better thermal transport. If there are two or more atomic layers in the thin film, it is found that R_F generally decreases with increasing ε_F. If ε_F is higher than 2, however, it is shown that the increase in ε_F has only a small effect on R_F. The simulation results shown in figure 3 clearly indicate that it is possible to significantly improve the thermal transport across a solid(A)/solid(B) interface of two highly mismatched materials by inserting a thin film between them. The minimum $R_F/R_S = 0.47$ is obtained in the case of a single-layer thin film with $\varepsilon_F = 0.25$.

To understand the mechanisms responsible for the variation of R_F with ε_F and film thickness, the vibrational density of states (VDOS) for surface atoms in solid A and solid B and atoms in different layers in the thin film are calculated from the Fourier transform of atomic velocity autocorrelation functions (VAF) [19]. The VAF is obtained from an equilibrium MD simulation of the same system at the temperature of 1.25 in the microcanonical ensemble. The calculated VDOSs for the systems with different ε_Fs and film thicknesses are shown in figure 4. It is found that the atoms at the two solid surfaces and in the thin film all vibrate primarily with reduced frequencies below 10. Therefore, we only show the VDOSs in the frequency range less than 10 in figure 4.

Due to the difference in atomic masses, the VDOSs of the surface atoms in solid A and in solid B mainly populate in frequencies ranging from 2 to 9 and from 0.5 to 3, respectively. The small overlap between the two VDOSs indicates that the thermal energy transport by elastic phonon scattering at the interface is very limited, which is responsible for the large interfacial thermal resistance R_S. As shown in figure 4, the VDOSs of surface atoms in the two solids are only slightly affected by the variations of thin film thickness and ε_F. On the other hand, the VDOSs of atoms in the thin film are strongly affected by ε_F and thin film thickness. Generally, with the increase of ε_F, the populated modes in VDOSs of the thin film gradually shift from the low frequency region to the high frequency region, and the VDOS distribution becomes broader. As the number of atomic layers in the thin film

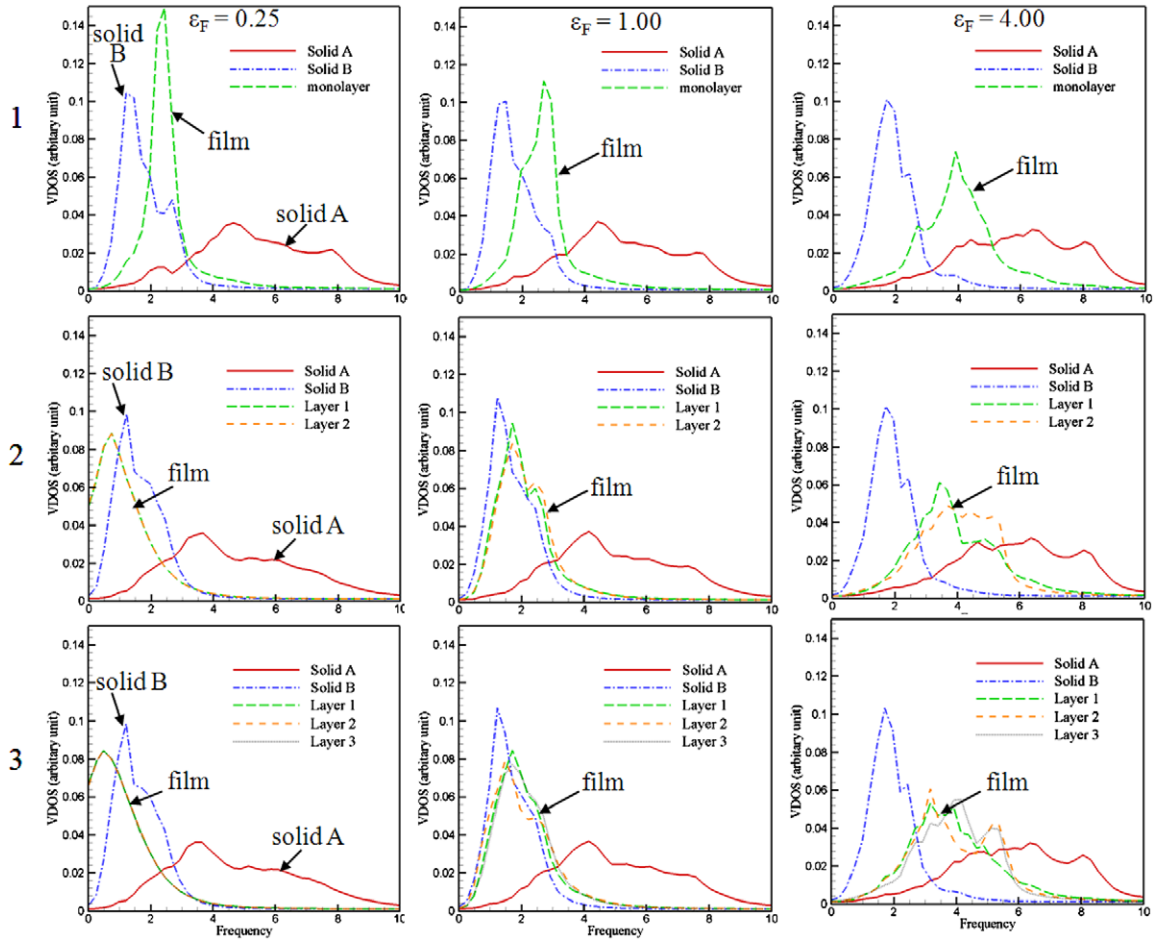

Figure 4. VDOS as a function of frequency for surface atoms in solid A (solid red lines) and solid B (blue dashed–dotted lines) and VDOSs of atoms in different layers of the thin film (counting from the solid(A)/film interface, first layer: green long-dashed lines; second layer: yellow dashed lines; third layer: black dotted lines) for a highly mismatched interface whose $R_S = 2.03$. first row: one-layer film; second row: two-layer film; third row: three-layer film; first column: $\varepsilon_F = 0.25$; second column: $\varepsilon_F = 1$; third column: $\varepsilon_F = 4$.

increases, the populated modes in VDOSs of the thin film shift slightly to the lower frequency region, and the shape of the VDOS curve becomes slightly broader.

As shown in figure 4, for a single-layer film with $\varepsilon_F = 0.25$, the overlap between the VDOSs of the thin film and solid B is almost as small as that between solid A and solid B. Therefore, it is not possible that the significant decrease in thermal resistance is cause by the increased elastic interface scattering. Hence, in the case of a single-layer film confined between two highly mismatched materials, we attribute the decrease in the interfacial thermal resistance to the increased inelastic phonon interface scattering. Since the VDOSs of atoms in solid A and in solid B mainly populate, respectively, in a high frequency region and a low frequency region, it is most likely that the atoms in the thin film facilitate the inelastic scattering of phonons, which means a phonon incident on the interface is scattered into two phonons with lower frequencies [20]. In this way, the thermal transport across the interface is greatly enhanced. Since R_F increases with ε_F for a single-layer film as shown in figure 3(c), the inelastic phonon scattering seems to be more likely to occur in single-layer thin films with lower binding energies.

On the other hand, for thin films containing two or more layers, the R_F of the thin film with a lower binding energy increases rapidly to a value higher than R_S, as shown in figure 3(b). For such thin films, the simulation temperature $T = 1.25$ is actually higher than their melting temperatures. The thermal transport in a liquid thin film is generally diffusive unless the thin film contains only one atomic layer [15]. As pointed out by Landry and McGaughey [9], the thin film thermal resistance in the diffusion limit is the sum of $R_{A/F}$, the thermal resistance at the solid(A)/film interface, $R_{B/F}$, the thermal resistance at the solid(B)/film interface, and R_{FC}, the thermal conductance resistance in the thin film, which is

$$R_F = R_{A/F} + R_{B/F} + R_{FC} \tag{3}$$

where R_{FC} generally increases with increasing film thickness. The rapid increase of R_F shown in figure 3(b) is attributed to the increase of thermal conduction resistance R_{FC} in the multi-layer film. As shown in figure 4, the VDOSs of the two-layer and three-layer films with low binding energies have nonzero populations at zero frequency. The VDOS at zero vibration frequency is proportional to the self-diffusion

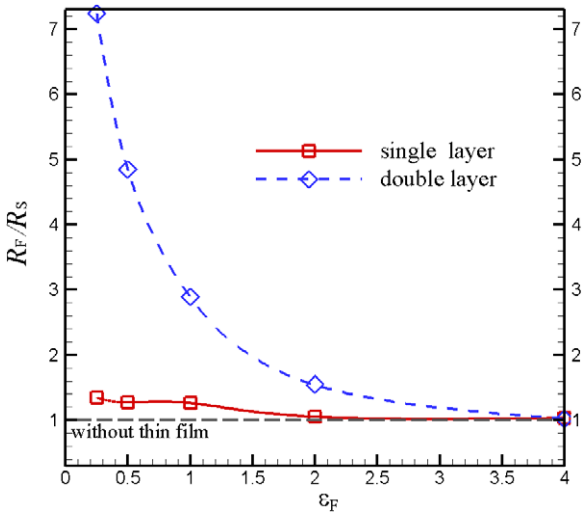

Figure 5. Thin film thermal resistance as a function of ε_F for a moderately mismatched interface whose $R_S = 0.47$. The uncertainty of R_F is less than the size of the symbols.

coefficient of atoms in the thin film. For solid materials, the atomic self-diffusion coefficient should be zero. The nonzero self-diffusion coefficient is a property of bulk fluid. Hence, the structure of a multi-layer thin film with low binding energies is fluid-like. Since the thermal conduction resistance of a fluid is normally orders of magnitude higher than that of a solid, it is reasonable to see the increase of R_F shown in figure 3(b).

For multi-layer thin films, it is found in figure 4 that the VDOSs of the thin films decrease from nonzero ($\varepsilon_F = 0.25$) to zero ($\varepsilon_F = 4.00$) at zero frequency. As ε_F increases, therefore, the self-diffusion coefficient of atoms in the thin film becomes zero which indicates that the structure of the thin film becomes solid-like. In this case, it is found that the VDOS distribution of the thin film has considerably large overlaps with the VDOS distribution of both solid A and solid B. The large overlaps indicate increased thermal transport by elastic phonon scattering at interfaces. Hence, a decrease of R_F with ε_F for multi-layer thin films is found in figure 3(c).

In the case of single-atom-layer film, the solid–film interactions dominate the motion of atoms in the thin film. With the increase of film thickness, the film–film interactions become more important. Accordingly, the VDOS of the thin film becomes more bulk-like and slightly broader, as shown in figure 4. A relatively sharp and narrow VDOS of the single-layer film should be caused by the strong confinement effect. The broader VDOS distribution increases the overlap between the thin film VDOS and the VDOSs of the two solids, which results in a slightly enhanced thermal transport by the increased elastic phonon scattering at both the solid(A)/film and solid(B)/film interfaces, which in contrast may decrease the inelastic interface scattering. Therefore, it is shown in figure 3(a) that R_F reaches a minimum at a certain film thickness and then increases with film thickness.

3.2. Thermal resistance at the moderately mismatched interface

To study the thermal transport across a moderately mismatched interface, we simply change m_B from 9 to 4, while fixing all other parameters of the solid A and solid B. Thus, $\sqrt{(\varepsilon_B/m_B)/(\varepsilon_A/m_A)} = 0.5$. From the MD simulation, it is found that $R_S = 0.47$ for an atomically perfect interface. Similarly, we fix $m_F = 2$ and vary ε_F from 0.25 to 4. Non-equilibrium MD simulations are carried out to determine R_Fs, while equilibrium MD simulations are also carried out to find VDOS for each ε_F. The calculated R_F as a function of ε_F is shown in figure 5. The VDOSs are shown in figure 6. In

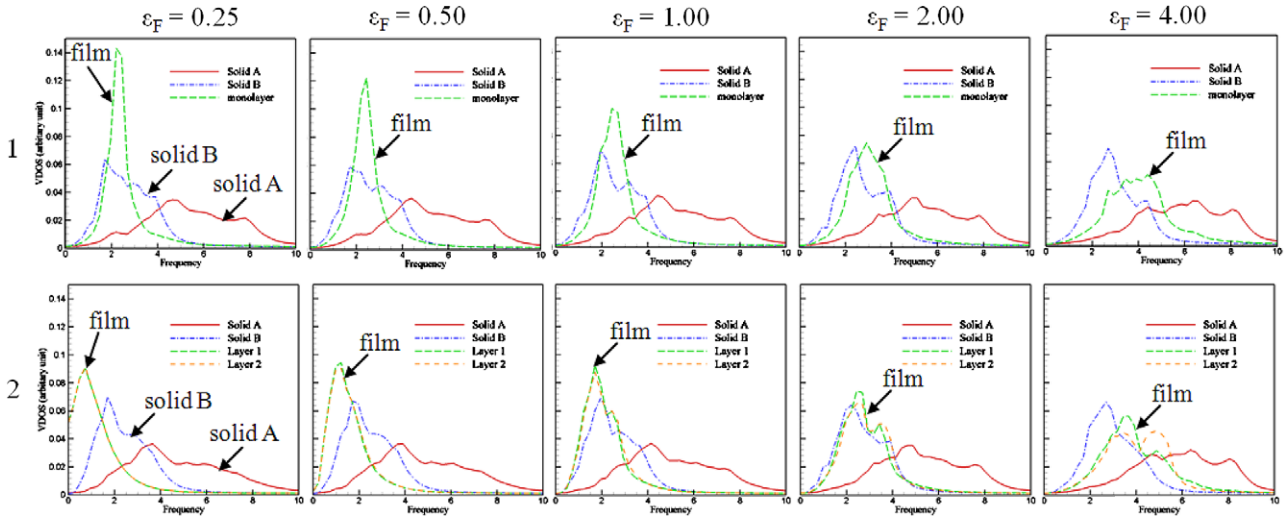

Figure 6. VDOS as a function of frequency for surface atoms in solid A (solid red lines) and solid B (blue dashed–dotted lines) and VDOSs of atoms in different layers of the thin film (counting from the solid(A)/film interface, first layer: green long-dashed lines; second layer: yellow dashed lines) for a moderately mismatched interface whose $R_S = 0.47$; first row: one-layer film; second row: two-layer film; first column: $\varepsilon_F = 0.25$; second column: $\varepsilon_F = 0.5$; third column: $\varepsilon_F = 1$; fourth column: $\varepsilon_F = 2$; fifth column: $\varepsilon_F = 4$.

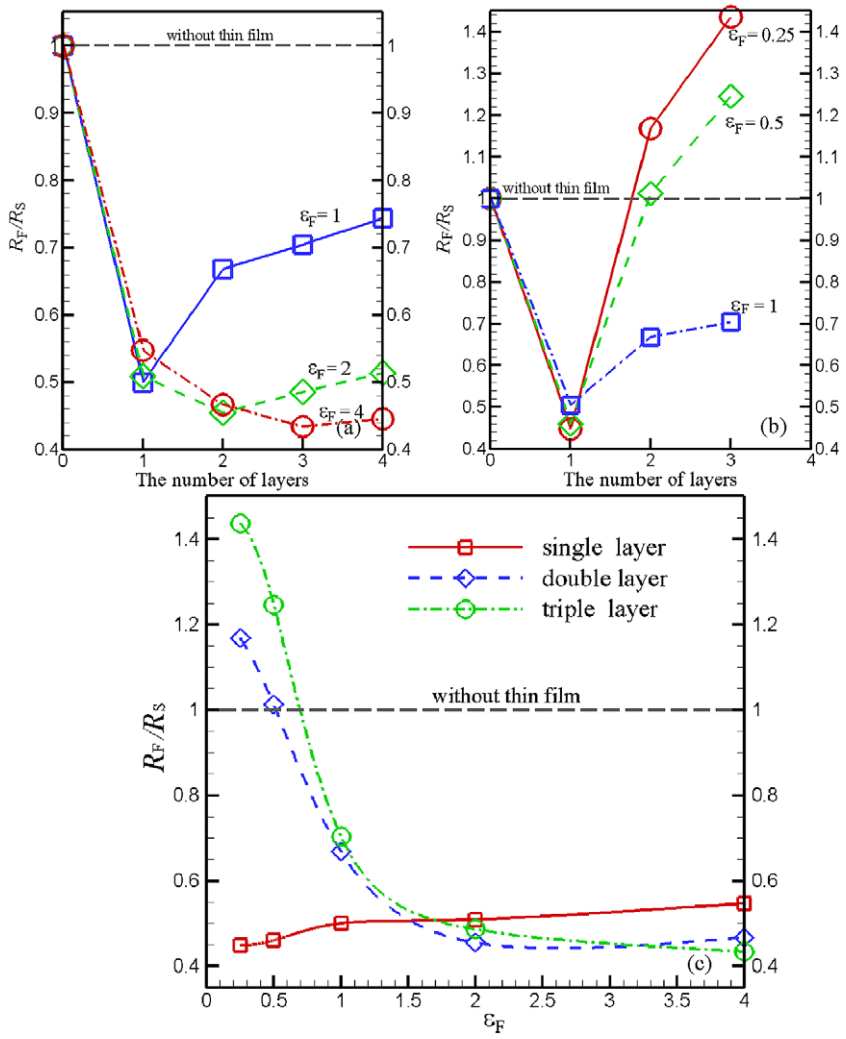

Figure 7. Thin film thermal resistance as a function of film thickness for (a) $\varepsilon_F = 1$, 2 or 4; (b) $\varepsilon_F = 0.25$, 0.5 or 1; and (c) thin film thermal resistance as a function of ε_F for a highly mismatched interface whose $R_S = 4.22$. The uncertainty of R_F is less than the size of the symbols.

this set of simulations, the measured q_Ss for different thin film parameters are mostly around 0.058.

Due to the relatively small mass ratio ($m_B/m_A = 4$), in figure 6 the VDOS distribution of the solid B has a larger overlap with that of the solid A, as compared to the results shown in figure 4. The larger overlap of VDOS distributions indicates the thermal transport across the interface by elastic phonon scattering becoming more important. It is seen from figure 5 that R_F decreases monotonically with ε_F for both the one-layer and two-layer films. All R_Fs in our calculations are found to be greater than R_S. As shown in figure 6, the overlap between the VDOS distributions of the thin film and solid A is smaller than that between the VDOS distributions of solid B and solid A, except for $\varepsilon_F = 4$. The smaller overlap of VDOSs indicates that the thermal transport by elastic interface scattering is reduced by insertion of a thin film. Although the insertion of a single-layer film has shown in the last section to be able to increase the thermal transport by increasing inelastic interface scattering, it cannot compete with the decrease of elastic interface scattering. In this case, the thermal transport contributed by the inelastic phonon scattering is less important in the moderately mismatched interface than in the aforementioned highly mismatched interface. Hence, it is reasonable to see that the insertion of a thin film does not improve the thermal transport across a moderately mismatched interface.

As ε_F increases, the VDOS of the thin film gradually shifts from a low frequency region to a higher frequency region and has an increasingly larger overlap with that of the solid A. The larger overlap thus increases the thermal transport contributed by elastic interface scattering and decreases R_F. Hence, the VDOSs shown in figure 6 explain the ε_F dependence of R_F shown in figure 5.

3.3. A comparison to interface mixing

The aforementioned MD simulation results are all obtained at a reduced temperature of 1.25 which is approximately one-half of the melting temperature of the solids. In [2], Stevens *et al* also calculated R_S using an LJ potential model at the solid–solid interface at a temperature approximately

one-half of the melting temperature of the material by MD simulations. Stevens *et al* found at a highly mismatched interface where $\sqrt{(\varepsilon_B/m_B)/(\varepsilon_A/m_A)} = 0.2$, it is possible to enhance the thermal transport by a factor of 1.8 ($R_S/R_{mix} = 1.8$) by systematically mixing atoms close to the interface with a mixing depth of 20 atomic layers. To compare with this result, we set $\varepsilon_A = 7$, $\varepsilon_B = 5$, $m_A = 0.5$ and $m_B = 9$ in our simulation so that $\sqrt{(\varepsilon_B/m_B)/(\varepsilon_A/m_A)} = 0.2$. All other parameters are the same as those used in the aforementioned MD simulations. For an atomically perfect solid(A)/solid(B) interface, R_S is found to be equal to 4.22. When a thin film is confined between the two solids, we calculate R_F as a function of ε_F and film thickness and show the results in figure 7. In this set of simulation, the measured q_Ss for different thin film parameters are mostly around 0.049. It is found that the variations of R_F with ε_F and film thickness are very similar to the results shown in figure 3 where $\sqrt{(\varepsilon_B/m_B)/(\varepsilon_A/m_A)} = 0.33$. The minimum thin film thermal resistance ($R_F = 1.85$) is found in the case of either a single-layer film with $\varepsilon_F = 0.25$ or a triple-layer film with $\varepsilon_F = 4$. Therefore, an enhancement of thermal transport by a factor of 2.3 ($R_S/R_F = 2.3$), as compared to a factor of 1.8 in the interface mixing case, is obtained by confining a thin film between two highly mismatched materials.

4. Conclusions

For a highly mismatched interface, the insertion of a thin film can greatly enhance the thermal transport across the interface. The maximum improvement of thermal transport can be achieved by inserting either a single-atom-thick film which is weakly bonded to the solids on either side of the thin film or a multi-atom-thick thin film which has high film–film and film–solid binding energies. The reduction of interfacial thermal resistance in the single-atom-layer film case is found mainly due to the increased inelastic scattering of phonons by atoms in the thin film. The improvement of thermal transport in the multi-atom-thick film case is found mainly due to the phonon DOS of the film which bridges the two different phonon DOSs on either side of the thin film. The improvement of thermal transport at a highly mismatched interface by inserting a thin film is found to be comparable to that via mixing the two mismatched materials by several atomic layers. For a moderately mismatched interface, however, the insertion of a thin film may decrease the thermal transport. The simulation results in this work may lead to improvements in the design of nanoscale components or devices which have specific thermal management requirements. The results in this work are all obtained at a temperature of approximately one-half of the melting temperature of the solids. Quantitatively different results may be obtained at higher or lower temperatures. Hence, the temperature-dependent results need further investigations.

Acknowledgments

We thank the National Institute for Computational Science (NICS) and the National Center for Supercomputing Applications (NCSA) for providing us with supercomputer resources for MD simulations.

References

[1] Cahill D G, Ford W K, Goodson K E, Mahan G D, Majumda A, Maris H J, Merlin R and Phillpot S R 2003 *J. Appl. Phys.* **93** 793
[2] Stevens R J, Zhigilei L V and Norris P M 2007 *Int. J. Heat Mass Transfer* **50** 3977
[3] Stoner R J and Maris H J 1993 *Phys. Rev.* B **48** 16373
[4] Chen G J 2001 *Heat Transfer* **123** 1
[5] Ni B, Watanabe T and Phillpot S R 2009 *J. Phys.: Condens. Matter* **21** 084219
[6] Liang X G and Sun L 2005 *Microscale Thermophys. Eng.* **9** 295
[7] Ju S, Liang X and Wang S 2010 *J. Phys. D: Appl. Phys.* **43** 085407
[8] Sun L and Murthy J Y 2010 *J. Heat Transfer* **132** 102403
[9] Landry E S and McGaughey A J H 2010 *J. Appl. Phys.* **107** 013521
[10] Lyeo H K and Cahill D G 2006 *Phys. Rev.* B **73** 144301
[11] Roberts D and Triplett G 2008 *Solid State Electron.* **52** 1669
[12] Li Y L, Huang Y R and Lai Y H 2007 *Appl. Phys. Lett.* **91** 181113
[13] Lombardo S, Stathis J H, Linder B P, Pey K L, Palumbo F and Tung C H 2005 *J. Appl. Phys.* **98** 121301
[14] Girit C O and Zettl A 2007 *Appl. Phys. Lett.* **91** 193512
[15] Liang Z and Tsai H L 2011 *Phys. Rev.* E **83** 061603
[16] Berendsen H J C, Postma J P M, Van Gunsteren W F, Di Nola A and Haak J R 1984 *J. Chem. Phys.* **81** 3684
[17] Jund P and Jullien R 1999 *Phys. Rev.* B **59** 13707
[18] Ohara T 1999 *J. Chem. Phys.* **111** 9667
[19] Allen M P and Tildesley D J 2000 *Computer Simulation of Liquid* (Oxford: Oxford University Press)
[20] Swartz E T and Pohl R O 1989 *Rev. Mod. Phys.* **61** 605